DOI: 10.1002/ejic.200800576

Synthesis, Protonation and Cu^{II} Complexes of Two Novel Isomeric Pentaazacyclophane Ligands: Potentiometric, DFT, Kinetic and AMP Recognition Studies

Andrés G. Algarra,[a] Manuel G. Basallote,*[a] Raquel Belda,[b] Salvador Blasco,[b] C. Esther Castillo,[a] José M. Llinares,[c] Enrique García-España,*[b] Laura Gil,[b] M. Ángeles Máñez,[a] Conxa Soriano,[c] and Begoña Verdejo[b]

Keywords: Cyclophanes / Macrocyclic ligands / Copper / Kinetics / Density functional calculations

The synthesis and coordination chemistry of two novel ligands, 2,6,9,12,16-pentaaza[17]metacyclophane (**L¹**) and 2,6,9,12,16-pentaaza[17]paracyclophane (**L²**), is described. Potentiometric studies indicate that **L¹** and **L²** form a variety of mononuclear complexes the stability constants of which reveal a change in the denticity of the ligand when moving from **L¹** to **L²**, a behaviour that can be qualitatively explained by the inability of the paracyclophanes to simultaneously use both benzylic nitrogen atoms for coordination to a single metal centre. In contrast, the formation of dinuclear hydroxylated complexes is more favoured for the *para* **L²** ligand. DFT calculations have been carried out to compare the geometries and relative energies of isomeric forms of the $[CuL]^{2+}$ complexes of **L¹** and **L²** in which the cyclophane acts either as tri- or tetradentate. The results indicate that the energy cost associated with a change in the coordination mode of the cyclophane from tri- to tetradentate is moderate for both ligands so that the actual coordination mode can be determined not only by the characteristics of the first coordination sphere but also by the specific interactions with additional nearby water molecules. The kinetics of the acid promoted decomposition of the mono- and dinuclear Cu^{II} complexes of both cyclophanes have also been studied. For both ligands, dinuclear complexes convert rapidly to mononuclear species upon addition of excess acid, the release of the first metal ion occurring within the mixing time of the stopped-flow instrument. Decomposition of the mononuclear $[CuL^2]^{2+}$ and $[CuHL^2]^{3+}$ species occurs with the same kinetics, thus showing that protonation of $[CuL^2]^{2+}$ occurs at an uncoordinated amine group. In contrast, the $[CuL^1]^{2+}$ and $[CuHL^1]^{3+}$ species show different decomposition kinetics indicating the existence of significant structural reorganisation upon protonation of the $[CuL^1]^{2+}$ species. The interaction of AMP with the protonated forms of the cyclophanes and the formation of mixed complexes in the systems Cu–**L¹**-AMP, Cu–**L²**-AMP, and Cu–**L³**-AMP, where **L³** is the related pyridinophane containing the same polyamine chain and 2,6-dimethylpyridine as a spacer, is also reported.

Introduction

In the last years some of us have focused on the synthesis and study of new families of cyclic ligands formed by linking together the ends of a polyamine and an aromatic spacer through methylene carbon atoms.[1–5] Perhaps one of the most interesting aspects of the coordination chemistry of these compounds is their ability to form metal complexes containing coordinatively unsaturated metal sites. In each case, the actual details of the coordination environments are affected by different factors such as the kind of aromatic spacer, the number of nitrogen atoms and the size and flexibility of the polyamine chain.

The role of the aromatic spacer, in particular the type of substitution (*ortho*, *meta* or *para*), becomes fundamental in the coordination chemistry of synthetic cyclophanes, especially in those with polyamine chains of small size. For example, the rigidity of the *p*-xylyl unit prevents the simultaneous participation of both benzylic nitrogen atoms in the coordination of a single metal ion which results in a higher tendency for the formation of dinuclear complexes than that exhibited by analogous ligands with *o*- or *m*-xylyl spacers.[2,6] In contrast, small and medium-sized cyclophanes with one *o*-xylyl spacer usually form only mononuclear complexes. The larger the size of the polyamine, the less drastic these changes are so that the coordination chemistry

[a] Departamento de Ciencia de Materiales e Ingeniería Metalúrgica y Química Inorgánica, Facultad de Ciencias, Universidad de Cádiz,
Apartado 40, Puerto Real, 11510 Cádiz, Spain
E-mail: manuel.basallote@uca.es
[b] Departamento de Química Inorgánica, Instituto de Ciencia Molecular, Universidad de Valencia,
Apartado Correos 22085, 46071 Valencia, Spain
E-mail: enrique.garcia-es@uv.es
[c] Departamento de Química Orgánica, Facultad de Farmacia, Universidad de Valencia,
Avda. Vicente Andrés Estellés s/n, 46100 Burjassot (Valencia), Spain
Supporting information for this article is available on the WWW under http://www.eurjic.org or from the author.

of these isomers becomes more similar. In the present work, we decided to analyse the case of the isomeric cyclophanes **L¹** and **L²** (see Figure 1), paying special attention to their behaviour towards protonation and to their ability to form mono- and dinuclear Cu^{II} complexes. In addition, the kinetic properties of the latter complexes have been also examined in order to obtain additional information about the lability of closely related metal complexes differing only in their protonation states. In this sense, recent reports have shown that the different CuH_xL^{z+} species of a given ligand can decompose with different kinetics which reveals the existence of extensive structural reorganisation of the Cu^{II} complexes upon protonation.[7] The paper also includes some exploratory work on the stability of the AMP species formed by the cyclophanes and their copper complexes. The nucleotide-recognition capability of protonated noncyclic and macrocyclic polyamines was discovered decades ago[8–13] and it has been exploited for nucleotide sensing and separation.[14–17] The interaction of the ammonium groups in the H_xL^{x+} species with the phosphate anions of adenosine-5′-monophophate (AMP), adenosine-5′-diphophate (ADP) and adenosine-5′-triphophate (ATP) leads to the formation of $H_xLA^{(x-z)+}$ (A^{z-} = nucleotide anion) species with increased stability as a consequence of π stacking interactions with aromatic rings in the polyamine. To gain insight into the stability of this kind of species, an initial approach to the nucleotide-recognition capability of the **L¹**–**L³** cyclophanes and their Cu^{II} complexes was made by studying their interaction with AMP.

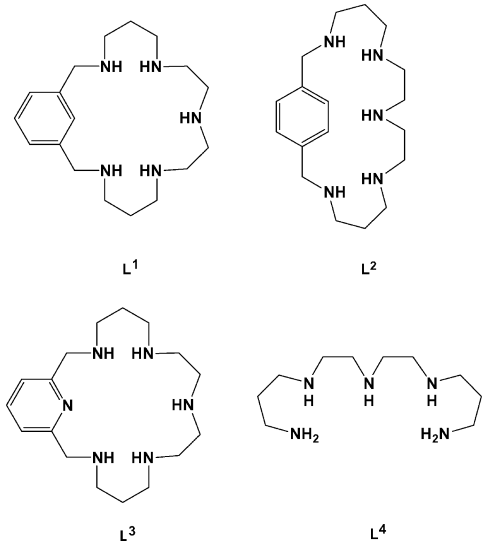

Figure 1. Ligands and abbreviations used in this work.

Results and Discussion

Equilibrium Studies on Ligand Protonation and Cu^{II} Complexation

The stepwise protonation constants for the **L¹** and **L²** ligands are included in Table 1 and compared with those previously reported for the open-chain counterpart **L⁴**[18] and the corresponding pyridine derivative **L³**.[19] In all cases the five expected protonation steps can be identified within the pH range of the study (2–11) and the trend in the values of the stepwise constants can be easily rationalised on the basis of minimisation of electrostatic repulsion between the positive charges generated at the protonated amine groups. Thus, the new **L¹** cyclophane shows large values of the constants for the first two protonation steps whereas the third and fourth protonation steps occur with constants with intermediate values and the last step occurs with a much more reduced protonation constant as a consequence of the fact that the incoming proton is forced to bind to the central nitrogen of the polyamine chain while being surrounded by two protonated sites separated by ethylenic chains. These results are quite similar to those previously reported for the analogous pyridinophane **L³**[19] for which the proposed protonation sequence was confirmed by ^1H and ^{13}C NMR spectroscopy at variable pH values. For these two ligands (**L¹** and **L³**), the protonation constants are always smaller than those corresponding to the open-chain **L⁴** ligand. In contrast, although the results obtained for **L²** are quite parallel, a greater basicity is observed for all the protonation steps in this ligand, probably because the *para* substitution at the aromatic spacer facilitates the separation of the positive charges generated at the cyclophane upon protonation. As a consequence of this capability, the protonation constants for **L²** become closer to those obtained for the open-chain polyamine **L⁴**.[18]

Table 1. Stepwise protonation constants for the **L¹** and **L²** ligands.[a] Literature values[18,19] for the protonation constants of **L³** and **L⁴** are also included for comparison.

Reaction[b]	**L¹**	**L²**	**L⁴**	**L³**
H + L = HL	9.70(2)	10.69(2)	10.55	9.65
H + HL = H_2L	9.37(2)	9.66(1)	9.89	9.32
H + H_2L = H_3L	7.81(2)	8.32(2)	8.69	7.62
H + H_3L = H_4L	6.99(2)	7.21(2)	7.55	6.62
H + H_4L = H_5L	2.80(4)	3.03(3)	3.55	2.86
log β_5	36.67	38.91	40.23	36.07

[a] At 298.1 K in the presence of 0.15 M $NaClO_4$. The values in parentheses correspond to the standard deviations in the last significant figure. [b] Charges omitted for clarity.

The stability constants for the formation of Cu^{2+} complexes with the **L¹** and **L²** cyclophanes are included in Table 2 together with those previously reported for **L³** and **L⁴**.[18,19] All three cyclophanes allow for the formation of both mono- and dinuclear metal complexes whereas the open-chain **L⁴** ligand only forms mononuclear species. As usually occurs in these kinds of ligands, the nuclearity of the species formed is strongly dependent on the M/L molar ratio so that while for **L¹** at a 1:1 ratio only mononuclear species are detected throughout the whole pH range studied, for a 2:1 ratio the dinuclear hydroxylated complex is the only species in solution above pH 6 (Figure 2). As expected from the change in the substitution at the aromatic spacer, the stability of the dinuclear species increases for the *para*-substituted **L²** cyclophane. For a 2:1 molar ratio several dinuclear species can be detected which also dominate the species distribution curves above pH 6 (Figure 3).

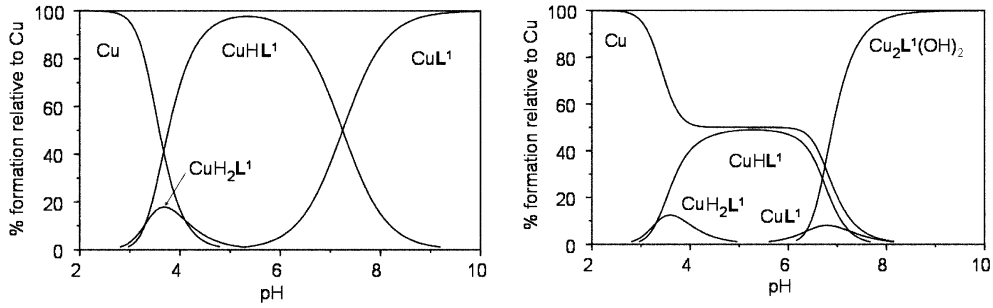

Figure 2. Distribution diagram for the system Cu^{2+}-$\mathbf{L^1}$. (A) $[Cu^{+2}] = [\mathbf{L^1}] = 10^{-3}$ mol dm^{-3}. (B) $[Cu^{+2}] = 2\times10^{-3}$ mol dm^{-3} $[\mathbf{L^1}] = 10^{-3}$ mol dm^{-3}.

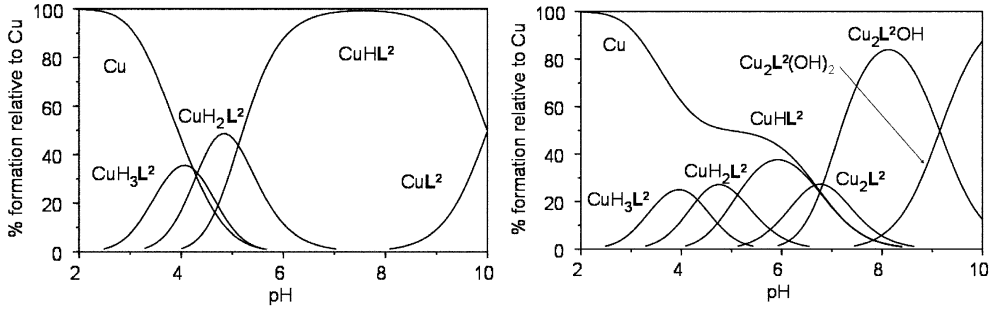

Figure 3. Distribution diagram for the system Cu^{2+}–$\mathbf{L^2}$. (A) $[Cu^{+2}] = [\mathbf{L^2}] = 10^{-3}$ mol dm^{-3}. (B) $[Cu^{+2}] = 2\times10^{-3}$ mol dm^{-3} $[\mathbf{L^2}] = 10^{-3}$ mol dm^{-3}.

Table 2. Stepwise stability constants for the formation of Cu^{2+} complexes with the $\mathbf{L^1}$ and $\mathbf{L^2}$ cyclophanes.[a] Literature values[18,19] for the systems Cu^{2+}-$\mathbf{L^3}$ and Cu^{2+}-$\mathbf{L^4}$ are also included for comparative purposes.

Reaction[b]	$\mathbf{L^1}$	$\mathbf{L^2}$	$\mathbf{L^3}$	$\mathbf{L^4}$
Cu + L = CuL	19.05 (1)	15.70(4)	20.44	21.28
CuL + H = CuHL	7.25 (3)	10.00(4)	6.96	8.86
CuHL + H = CuH_2L	3.33 (2)	5.12(2)	2.75	3.39
2 Cu + L = Cu_2L	–	22.00(6)	–	–
2 Cu + L + H_2O = $Cu_2L(OH)$ + H	–	15.19(2)	20.65	–
2 Cu + L + 2 H_2O = $Cu_2L(OH)_2$ + 2 H	9.05 (1)	6.04(3)	10.84	–

[a] At 298.1 K in the presence of 0.15 M $NaClO_4$. The values in parentheses correspond to the standard deviations in the last significant Figure. [b] Charges omitted for clarity.

With regards to the actual values of the stability constants, the major observation made from the values in Table 2 is that the stability of the $[Cu\mathbf{L^2}]^{2+}$ species is significantly lower than that found for the same species with the other ligands suggesting a lower coordination number of the cyclophane in this case. The previously reported crystal structure of the $[Cu\mathbf{L^3}]^{2+}$ complex reveals a very distorted octahedral coordination sphere about the metal centre so that the coordination number of the ligand can be best described as being four.[19] A coordination number of four has also been established for the Cu^{II} complex of the acyclic $\mathbf{L^4}$ ligand.[19,20] Although deriving coordination numbers by taking into account only free energy terms can be misleading, a careful consideration of the stability constants of the different protonated and nonprotonated complex species, in comparison with the protonation of the free ligands, can provide some valuable information. In this sense, Table 2 reveals that the first protonation constant for the $[Cu\mathbf{L^1}]^{2+}$, $[Cu\mathbf{L^2}]^{2+}$ and $[Cu\mathbf{L^3}]^{2+}$ complexes has values that compare well with the third protonation step of the free ligands seen in Table 1, a step in which there are the same charge changes. This comparison suggests that not all the nitrogen atoms in the ligand are involved in metal coordination, as confirmed by the crystal structure for the case of $\mathbf{L^3}$ commented on above. However, the formation constant of $[Cu\mathbf{L^2}]^{2+}$ is much smaller than that obtained for the equivalent $\mathbf{L^3}$ species. This fact, and the high value for the second protonation constant for $[Cu\mathbf{L^2}]^{2+}$ strongly suggests that in this case there are only three nitrogen atoms tightly bound to the metal ion which contrasts with the tetradentate coordination observed for the $\mathbf{L^3}$–Cu complex.[19] Therefore, *p*-substitution at the aromatic ring of $\mathbf{L^2}$ appears to prevent the simultaneous participation of both benzylic nitrogen atoms in the coordination to a single metal ion, a conclusion supported by several previous reports of crystal structures involving *para*-azacyclophanes.[2–4]

In attempts to obtain additional information about the denticity of the $\mathbf{L^1}$ and $\mathbf{L^2}$ cyclophanes in their Cu^{II} complexes by using experimental techniques different from potentiometric data, were carried out instead EPR and UV/Vis spectroscopic studies. EPR spectra recorded at the pH values where the mononuclear species $[CuH\mathbf{L^1}]^{3+}$, $[Cu\mathbf{L^1}]^{2+}$, $[CuH\mathbf{L^2}]^{3+}$ and $[Cu\mathbf{L^2}]^{2+}$ predominate in solution (see some representative examples in the Supporting Information) are in all cases very similar to each other and they do not show any superhyperfine structure due to interaction with ^{14}N nuclei so that no direct information about the number of coordinated nitrogen atoms could be obtained. However,

since it has been reported that there is an approximate additivity of the influence of the number of nitrogen donors on the parameters in the EPR spectra of Cu-polyamine complexes,[21] a more detailed analysis of the EPR spectra at 100 K was made. The only species with an EPR spectrum significantly different from the other species is $[CuH\mathbf{L^2}]^{3+}$ and this shows an isotropic spectrum with a g value of 2.09 which suggests that protonation of $[Cu\mathbf{L^2}]^{2+}$ leads to a change in the geometry towards a tetrahedral structure. However, it was found that the spectra of the $[CuH\mathbf{L^1}]^{3+}$, $[Cu\mathbf{L^1}]^{2+}$ and $[Cu\mathbf{L^2}]^{2+}$ complexes are similar in all cases with values of $g_{\perp} = 2.08$, $g = 2.21$ and $A = 190$ G. These values compare well with those reported for $Cu(en)_2^{2+}$, $Cu(trien)^{2+}$ and $Cu(cyclam)^{2+}$[21] but no conclusions about differences in the denticity of the ligand in the $\mathbf{L^1}$ and $\mathbf{L^2}$ complexes could be established. Nevertheless, further evidence for the change in the denticity of the $\mathbf{L^1}$ and $\mathbf{L^2}$ ligands in their Cu complexes is provided by the electronic spectra which show an absorption maximum centred at 570 nm in the case of $[HCu\mathbf{L^1}]^{+3}$ ($\varepsilon = 194\ M^{-1}cm^{-1}$), 565 nm for $[Cu\mathbf{L^1}]^{2+}$ ($\varepsilon = 191\ M^{-1}cm^{-1}$), 585 nm for $[HCu\mathbf{L^2}]^{3+}$ ($\varepsilon = 85\ M^{-1}cm^{-1}$), 585 nm for $[Cu\mathbf{L^2}]^{2+}$ ($\varepsilon = 110\ M^{-1}cm^{-1}$) and 610 nm for $[Cu_2\mathbf{L^2}(OH)]^{3+}$ ($\varepsilon = 215\ M^{-1}cm^{-1}$). A maximum at wavelengths close to 575 nm has been observed for complexes with related polyamines acting as tetradentate ligands with four coordinated nitrogen atoms disposed at the vertices of a square around the metal ion whereas complexes with tridentate polyamines show absorption bands at larger wavelengths, close to that found for $[Cu\mathbf{L^2}]^{2+}$. Thus, the $Cu(dien)^{2+}$ complex shows a maximum at 605–615 nm ($\varepsilon = 73$–$82\ M^{-1}cm^{-1}$)[20] and the H_3CuL complex of 4,7,10,13-tetraazahexadecane-1,16-diamine shows its maximum at 590 nm (ε not given in the literature).[18] Both of these complexes contain a polyamine coordinated in a tridentate manner and coordination of an additional amine group leads to a shift of the maximum to shorter wavelengths by 15–60 nm relative to the 3 N coordinated species: $Cu(dien)(NH_3)^{2+}$ has $\lambda_{max} = 576$ nm ($\varepsilon = 84\ M^{-1}cm^{-1}$),[20] for the CuL^{2+} complex of 4,7,10,13-tetraazahexadecane-1,16-diamine $\lambda_{max} = 578$ nm ($\varepsilon = 178\ M^{-1}cm^{-1}$)[18] and for the $HCuL^{3+}$ and CuL^{2+} species with 4,7,10-triazatridecane-1,13-diamine the values are $\lambda_{max} = 573$ nm ($\varepsilon = 187\ M^{-1}cm^{-1}$) and $\lambda_{max} = 585$ nm ($\varepsilon = 214\ M^{-1}cm^{-1}$),[20] respectively. Interestingly, increased molar absorptivities were also observed in the tetracoordinated species ($\varepsilon = 170$–$200\ M^{-1}cm^{-1}$) with respect to the corresponding tricoordinated species ($\varepsilon = 70$–$150\ M^{-1}cm^{-1}$), something which was attributed to distortion from an ideal square planar structure.[20]

Another important point to consider is the formation of dinuclear hydroxy complexes. Since these ligands do not saturate the first coordination sphere of two metal ions, the metal centres must bind other ligands which should most likely be water molecules in the absence of better entering ligands. However, because of the electrostatic repulsion between the metal centres, hydrolysis of coordinated water to form μ-hydroxo species is favoured, the major species in solution being $[Cu_2\mathbf{L^1}(OH)_2]^{3+}$ above pH 7, $[Cu_2\mathbf{L^2}(OH)]^{3+}$ above pH 7 and $[Cu_2\mathbf{L^2}(OH)_2]^{2+}$ above pH 9. The low pK_a value for the reaction of $[Cu_2\mathbf{L^2}]^{4+}$ to give $[Cu_2\mathbf{L^2}(OH)]^{3+}$ ($pK_a = -6.82$) suggests that the hydroxo ligand might be bridging both metal centres. From the behaviour of related compounds, it can be anticipated that these dinuclear species can show interesting properties in the assistance of hydrolytic processes with different electrophilic substrates such as carboxylates or phosphates,[5,22] a possibility that will be explored in future work.

DFT Calculations on the Formation of CuL^{2+} Species with the L^1 and L^2 Ligands

The most striking result in the previous section is probably the large difference in the stability constants of the $[Cu\mathbf{L^1}]^{2+}$ and $[Cu\mathbf{L^2}]^{2+}$ complexes which strongly suggests a change in the number of donor atoms used by the cyclophane in both complexes with $\mathbf{L^1}$ acting as tetradentate and $\mathbf{L^2}$ as tridentate. In addition, potentiometric results do not provide any evidence of coordination of these ligands through the whole set of five potential nitrogen donors in any of the species formed in solution. While the latter findings can be rationalised by invoking the steric constraints imposed by the aromatic spacer, there is no apparent reason to think that any of these cyclophanes could not behave as a tetradentate ligand in their Cu^{II} complexes and we therefore think that the reasons for the tridentate behaviour of $\mathbf{L^2}$ must be related to the stability difference between species with the ligand acting as tri- and tetradentate. For this reason, we carried out DFT calculations aimed at determining the geometries and relative energies of $[Cu\mathbf{L}]^{2+}$ species containing both tridentate and tetradentate $\mathbf{L^1}$ or $\mathbf{L^2}$. As expected from the equilibrium measurements, all attempts to optimise the geometries of species with the ligand acting as pentadentate were unsuccessful because the optimisation procedure leads to dissociation of at least one Cu–N bond. In addition, the calculations confirmed the expectations in the sense that the possibility of a first coordination sphere involving both benzylic nitrogen atoms is, in the case of $\mathbf{L^2}$, prevented due to geometric constraints.

The optimised geometries and relative energies of the most stable species found for the $[Cu\mathbf{L^1}]^{2+}$ and $[Cu\mathbf{L^2}]^{2+}$ complexes are shown in Figure 4 and Table 3 which include a set of structures that can be classified in all cases as distorted square pyramidal or tetragonally distorted octahedral, with Cu–N distances that fall within the 2.0–2.2 Å range. This kind of distorted geometry has been found in the crystal structures of many Cu^{II}–polyamine complexes, the experimental Cu–N distances being in all cases ca. 2.0–2.1 Å.[23,24] Another common feature of the calculated structures in Figure 4 is the existence of relatively large Cu–O distances with the axially coordinated water molecules. This elongation of the axial bonds is also quite common in the crystal structures of Cu-polyamine complexes, although the experimental distances tend to be smaller than those calculated by the DFT procedures.[25] However, it must be pointed out that the DFT calculations indicate that the in-

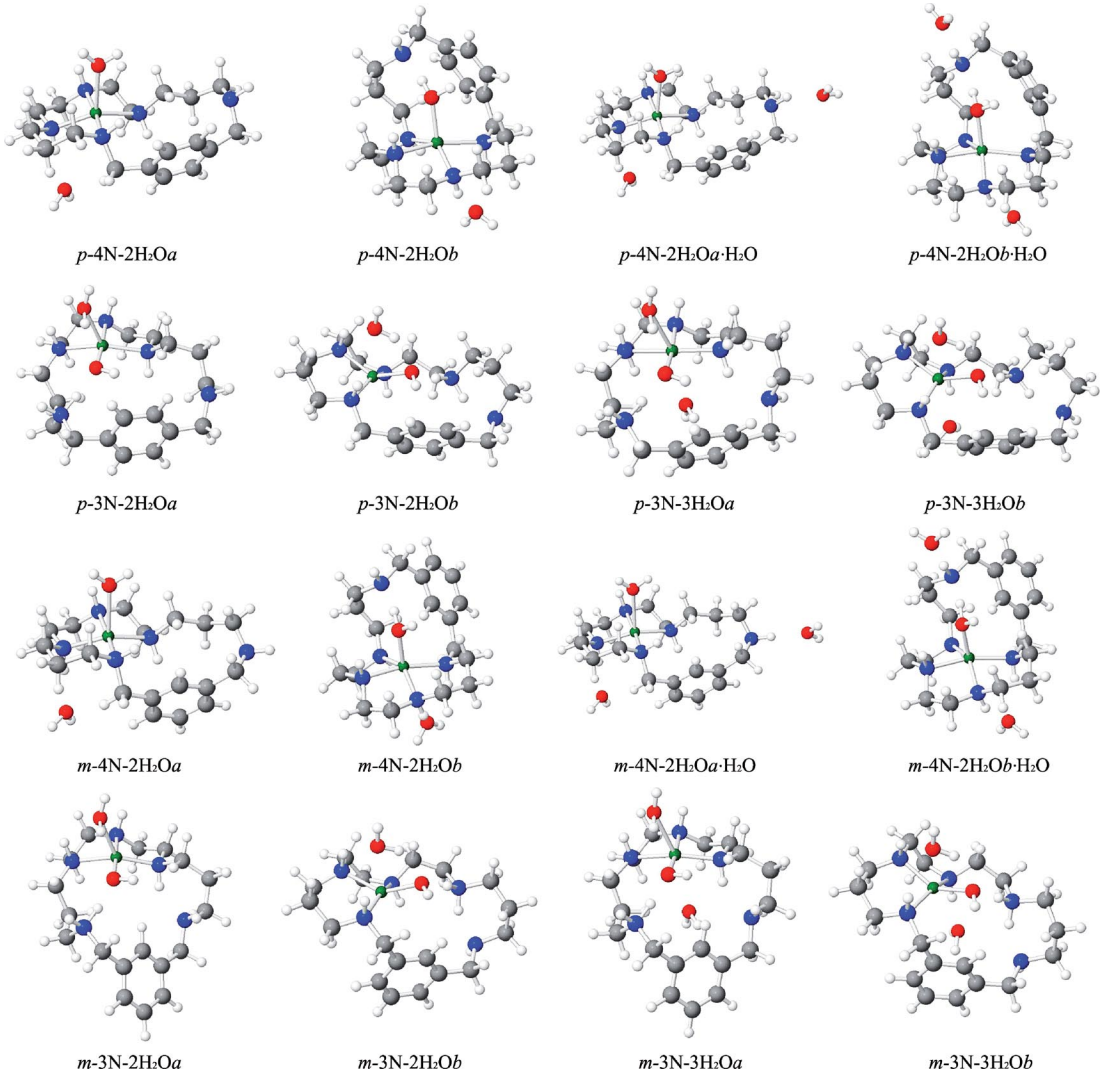

Figure 4. Optimised geometries calculated for the $[CuL^1]^{2+}$ and $[CuL^2]^{2+}$ complexes with the cyclophane acting as tri- or tetradentate. Colour code: green Cu, red O, blue N, grey C, white H.

teraction of the metal ion with the axial ligand is very weak so that relatively large changes in the bond lengths lead to small energy changes. Under these conditions, it must be expected that the actual bond lengths in solution and in the crystals will be strongly dependent on factors such as solvation, hydrogen bonding and crystal packing forces.

Optimised geometries calculated for the $[CuL^1]^{2+}$ or $[CuL^2]^{2+}$ complexes with the cyclophanes acting as tri- or tetradentate ligands are collected in Figure 4. We will first discuss the structures of the pentacoordinated complexes with three central nitrogens of the bridge and two water molecules (structures *m*-3N-2H_2O*a* and *p*-3N-2H_2O*a* in Figure 4). For both cyclophanes, the complexes display a distorted square pyramidal coordination with the three coordinated amine groups located in the basal plane and one of the coordinated waters forming a strong hydrogen bond with one of the uncoordinated benzylic nitrogen atoms. From these structures, a third water molecule was included in the calculations and located in the vacant coordination site opposed to the apical water. The calculations lead to structures (*m*-3N-3H_2O*a* and *p*-3N-3H_2O*a*) that show a very distorted octahedral geometry with one of the axial water ligands placed significantly closer to the metal ion than the other (Cu–O distances of 2.48 and 3.20 Å for *m*-3N-3H_2O*a*, and 2.54 and 2.84 Å for *p*-3N-3H_2O*a*). As in

Table 3. Relative energy (kcal mol^{-1}) of the different species calculated for the Cu^{II} complexes with the L^1 and L^2 ligands (see optimised structures in Figure 4).

Species	L^1 (*m*) Gas phase	Aqueous solution	L^2 (*p*) Gas phase	Aqueous solution
3N-2H_2O*a* + H_2O	0.0	0.0	0.0	0.0
3N-2H_2O*b* + H_2O	0.9	6.4	–6.0	1.2
3N-3H_2O*a*	–11.6	–2.0	–15.3	5.1
3N-3H_2O*b*	–14.8	1.4	–20.4	–3.8
4N-2H_2O*a* + H_2O	9.6	6.5	5.9	5.6
4N-2H_2O*b* + H_2O	15.4	15.2	14.6	25.0
4N-2H_2O*a*·H_2O	0.2	4.7	–3.7	4.0
4N-2H_2O*b*·H_2O	0.8	9.8	12.6	22.4

the previous structures, the water in the equatorial plane forms a strong hydrogen bond with one benzylic nitrogen. As expected from its weak interaction with the metal ion, the stabilisation associated with the third water molecule is not large, so that the structures *m*-3N-3H_2O*a* and *p*-3N-3H_2O*a* are only 2.0 and –5.1 kcal mol^{-1} more stable in aqueous solution than a separate water molecule and *m*-3N-2H_2O*a* or *p*-3N-2H_2O*a*, respectively (11.6 and 15.3 kcal mol^{-1} in the gas phase). These differences are expected to be even smaller in real systems because of the possibility of hydrogen bonding between the third water and the *m*-3N-2H_2O*a* or *p*-3N-2H_2O*a* species.

Figure 4 also includes the optimised geometries for pentacoordinate complexes with tridentate cyclophane but with a coordination environment that includes one of the benzylic nitrogen donors. These species are named following the procedure in the previous paragraph except that they are labelled as *b* instead of *a*. Their optimised structures can be described in a parallel way to that used for the *a* family and the relative energies are also included in Table 3. It is interesting to note that the species in the *b* family are less stable than their analogues with the other coordination mode (*a* series) in the case of the **L¹** complexes but they are more stable in the case of **L²**.

Finally, Figure 4 includes the optimised geometries for species containing tetradentate **L¹** and **L²**. The only way of obtaining stable structures with this coordination was by keeping one of the benzylic nitrogen atoms uncoordinated, all attempts with all the nitrogen atoms coordinated except one of the central amine groups being unsuccessful. For this coordination, two different geometries close in energy could be optimised for each of the cyclophanes. In the structures of *m*-4N-2H_2O-*a* and *p*-4N-2H_2O-*a*, one of the water molecules is displaced from the hypothetical sixth coordination site and forms a hydrogen bond with one of the coordinated amines in the equatorial plane. The distance from this water molecule to the metal centre is so large (4.0 Å for **L¹** and 3.9 Å for **L²**) and the H_2O–Cu–OH_2 angle deviates so much from 180° (actual values of 148.5 and 156.7° for **L¹** and **L²**, respectively) that the structures can be described as being pentacoordinate. However, these structures are not far in energy from the alternative *m*-4N-2H_2O-*b* and *p*-4N-2H_2O-*b* structures which show coordination environments with the four nitrogen atoms in the equatorial plane, one axial water located at 2.24 Å (**L¹**) or 2.16 Å (**L²**) and a weakly interacting water molecule located at 3.41 Å (**L¹**) or 3.70 Å (**L²**). The H_2O–Cu–OH_2 angle is now closer to 180° (actual values of 163.2 and 157.5° for **L¹** and **L²**, respectively). The energy difference between the *a*-*b* pairs of structures is significantly different for both ligands, those labelled as *a* being more stable by 8.7 (**L¹**) or 19.4 (**L²**) kcal mol^{-1} in solution (5.8 or 8.7 kcal mol^{-1} in the gas phase). As a whole, these results indicate that the stabilisation associated with this weak axial coordination of the second water molecule is lower than that associated with hydrogen bonding with one of the coordinated amine groups so that it is not expected to be coordinated in solution, especially in the case of **L²**.

With regards to the relative energies of the optimised geometries containing tri- and tetradentate cyclophanes, the results of the DFT calculations indicate in all cases a higher stability of the structures with the tridentate cyclophane, the energy difference between the 3N-3H_2O and 4N-2H_2O structured (plus a free additional H_2O) being 8.5 (**L¹**) or 0.5 (**L²**) kcal mol^{-1} in aqueous solution (20.0 and 21.2 kcal mol^{-1} in the gas phase, respectively) if the *a* series is considered in both cases. These differences are sure to be overestimates because of the possibility of hydrogen bonding between the third water molecule and the 4N-2H_2O systems and, for this reason, the systems were optimised whilst allowing for this interaction. The resultant geometries are also included in Figure 4 and labelled as *m*- or *p*-4N-2H_2O·H_2O. The species with tridentate cyclophanes are still more stable even when this additional interaction is considered in the tetradentate systems, although the energy difference is reduced. A similar conclusion can be drawn by comparing the energies of the 3N-2H_2O and 4N-2H_2O pairs of structures which also indicates a higher stability of the tridentate form.

In any case, it must be concluded from the DFT calculations that the energy difference between the different coordination modes is small for both cyclophanes and the actual values in real systems will be strongly dependent on the extent of hydrogen bonding with additional water molecules, something not considered in the calculations. From this point of view, both coordination modes are expected to coexist in solution. Moreover, since there are no large differences between the results obtained for the **L¹** and **L²** ligands, it must also be concluded that the experimental observation of tridentate coordination in $[Cu\mathbf{L^2}]^{+2}$ and tetradentate coordination in $[Cu\mathbf{L^2}]^{+2}$ cannot be attributed principally to changes in the first coordination sphere but must be better related to differences in the network of hydrogen bonds formed with uncoordinated water molecules. At this point, it is important to remember that the analysis of potentiometric results only provides direct information on the stoichiometry, Cu−L−H in the present case, and the stability of the different species but it does not allow a distinction to be made between isomeric species with the same stoichiometry, i.e. the stability constant derived for a species such as $[Cu\mathbf{L}]^{2+}$ does not discriminate between the possible relative contributions of microscopic species with the same stoichiometry but differing in the denticity of the ligand or in the number of coordinated water molecules. The results of the present DFT studies indicate that mixtures of species with different structures and even with a different denticity of the ligand can be formed in solution and that the relative amounts of each species are strongly dependent not only on the characteristics of the first coordination sphere but also on factors as difficult to quantify as the specific interactions with solvent molecules. In any case, despite the fact that calculations fail to predict the tetradentate behaviour of the cyclophane in $[Cu\mathbf{L^1}]^{2+}$, the calculations indicate that a higher stability of the tridentate form is expected to occur when changing to the *para* **L²** ligand. Inspection of the data in Table 3 reveals that changing from **L¹** to **L²** does not

change very much the energy of the most stable tetradentate form but it leads to stabilisation of all the tridentate forms, especially those involving coordination of one benzylic nitrogen, in agreement with the tridentate coordination mode found in the crystal structure of the Hg^{II} complex with a related cyclophane.[2b]

Kinetics of Decomposition of the Cu^{II} Complexes with the L^1 and L^2 Ligands

The species distribution curves in Figure 2 and Figure 3 show that upon addition of an excess of acid, the Cu–$\mathbf{L^1}$ and Cu–$\mathbf{L^2}$ complexes decompose with formation of Cu^{2+} and the fully protonated ligands, as indicated in Equation (1) for the case of a mononuclear species.

$$CuH_xL^{(2+x)+} + H^+_{exc} \rightarrow Cu^{2+} + H_5L^{5+} \quad (1)$$

Stopped-flow experiments showed that the acid promoted decomposition of the Cu^{II} complexes with both cyclophanes occurs in all cases with a single measurable kinetic step with rate constants that change with the acid concentration according to the rate law in [Equation (2)] (Figures 5 and 6). However, whereas for the $\mathbf{L^2}$ complexes the values of the observed rate constants are independent of the nature of the species in the starting solution (Figure 5) and the whole set of data can be well fitted by Equation 2 to obtain values of $a = 17.5 \pm 0.3\ s^{-1}$ and $b = 114 \pm 9\ M^{-1}s^{-1}$, the kinetic data for the $\mathbf{L^1}$ complexes change significantly for the different species studied (Figure 6). The values of the a and b parameters for each species are: $a = 24.7 \pm 0.1\ s^{-1}$ and $b = 119 \pm 2\ M^{-1}s^{-1}$ for $[CuH\mathbf{L^1}]^{3+}$, $a = 17.0 \pm 0.5\ s^{-1}$ and $b = 114 \pm 14\ M^{-1}s^{-1}$ for $[Cu\mathbf{L^1}]^{2+}$, and $a = 13.3 \pm 0.3\ s^{-1}$ and $b = 23 \pm 8\ M^{-1}s^{-1}$ for $[Cu_2\mathbf{L^1}(OH)_2]^{2+}$.

$$k_{obs} = a + b[H^+] \quad (2)$$

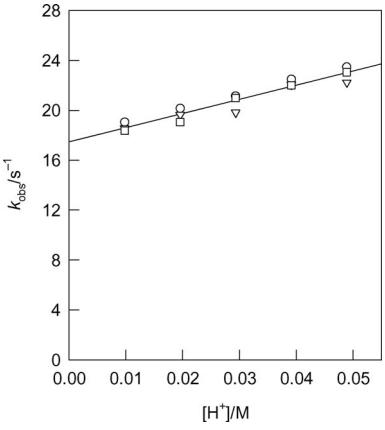

Figure 5. Plot of the observed rate constants vs. the acid concentration for the decomposition of the Cu^{II} complexes with $\mathbf{L^2}$ (25.0 °C, 0.15 M $NaClO_4$). The solid line corresponds to the best fit of all the data in the plot.

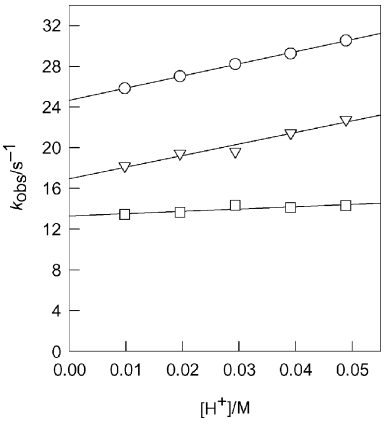

Figure 6. Plot of the observed rate constants vs. the acid concentration for the decomposition of the different Cu–$\mathbf{L^1}$ complexes (25.0 °C, 0.15 M $NaClO_4$): $[CuH\mathbf{L^1}]^{3+}$ (circles), $[Cu\mathbf{L^1}]^{2+}$ (triangles) and $[Cu_2\mathbf{L^1}(OH)_2]^{2+}$ (squares).

The spectra of the reaction mixture immediately after mixing in the stopped-flow instrument (ca. 2 ms) and at the end of the reaction were also recorded in all cases from the analysis of kinetic experiments using a diode-array detector and they were compared with those of the complex species before addition of the excess acid. Some representative spectra are shown in Figure 7 which includes the spectrum of the dinuclear $[Cu_2\mathbf{L^2}(OH)]^{3+}$ species in the absence of added acid (a) and the initial (b) and final (c) spectra in the kinetic experiments. These spectra clearly reveal the existence of a rapid absorbance change that occurs within the mixing time of the stopped-flow instrument. This initial fast absorbance change is only observed when the starting solution contains a dinuclear species, no rapid changes of similar characteristics being observed for the mononuclear species. Actually, the analysis of the spectroscopic changes observed during the decomposition of the mononuclear $[CuH\mathbf{L^2}]^{3+}$ and $[Cu\mathbf{L^2}]^{2+}$ species leads to initial and final spectra similar to those in Figure 7 (b) and Figure 7 (c). It is also interesting to note that dissociation of the first metal ion from the dinuclear $[Cu_2\mathbf{L^2}(OH)]^{3+}$ species does not cause any significant change in the position of the absorption maximum despite the fact that the hydroxyl bridge must be destroyed in the process. Nevertheless this observation is in agreement with the conclusions derived from the analysis of the spectra obtained at different pH and Cu/L ratios. As the rate constants obtained for the different Cu–$\mathbf{L^1}$ species are significantly different, special care was taken in this case to compare the spectra obtained for each species immediately after mixing with the acid excess. A rapid release of one Cu^{II} ion within the mixing time of the stopped-flow instrument was also observed during the decomposition of the dinuclear $[Cu_2\mathbf{L^1}(OH)_2]^{2+}$ species and in all cases an absorption maximum centred at wavelengths close to 570 nm was observed during the early stages of the stopped-flow experiment which suggests a similar coordination environment for the metal ion in all the three mononuclear Cu–$\mathbf{L^1}$ species, the decomposition kinetics of which lead to the rate constants in Figure 6.

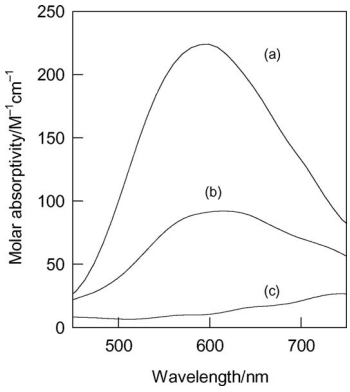

Figure 7. Comparison of the electronic spectrum of the $[Cu_2\mathbf{L^2}(OH)]^{3+}$ species (a) with the spectra obtained from the analysis of the spectroscopic changes recorded during the acid-promoted decomposition of this species: initial spectrum (b) and final product (c).

As a summary, the kinetics results indicate that decomposition of the mononuclear Cu^{II} complexes with both cyclophanes occurs in a single step, whereas the dinuclear species decompose in two steps, the first metal ion being released much faster than the second. Unfortunately, dissociation of the first Cu^{II} occurs within the mixing time of the instrument and no kinetic data could be obtained. It is important to note that the decomposition of the dinuclear complexes formed with larger polyaza macrocycles and cryptands occurs with a lower rate and statistically controlled kinetics, i.e. both metal centres behave independently and the rate of release of the first metal ion doubles the rate corresponding to the second.[26–29] Thus, it appears that the smaller size of the $\mathbf{L^1}$ and $\mathbf{L^2}$ cyclophanes creates important electrostatic repulsions between the metal centres in the dinuclear species and this results in the faster release of one metal ion upon treatment with acid.

The similarity of the spectroscopic changes and rate constants for the only measurable kinetic step for all the mono- and dinuclear Cu–$\mathbf{L^2}$ species strongly suggests that the same process is monitored in all cases which is surely the decomposition of the most acidic mononuclear species. These results for the $\mathbf{L^2}$ complexes can be easily rationalised by considering that the cyclophane does not use all the donor groups in the mononuclear complexes and the different species studied only differ by the protonation/deprotonation of some of the uncoordinated amine groups. In that case, addition of an excess of acid leads to the rapid protonation of the amine groups which remain uncoordinated and deprotonated. As a consequence, the species formed within the mixing time of the stopped-flow instrument is always the same and so the same kinetics of decomposition are observed independent of the starting species.

In contrast, the results obtained for the $\mathbf{L^1}$ complexes cannot be explained in the same way. The three different Cu–$\mathbf{L^1}$ mononuclear species, including that resulting from dissociation of the first ion from the dinuclear complex, decompose with different kinetics despite the fact that their spectra are also very similar in all cases. This similarity of the electronic spectra for the different species indicates a similar coordination environment of the metal ion, i.e. the number of donor groups used by the ligand must be the same in all cases independent of the protonation state of the complex. From the position of the absorption band, a tetradentate binding mode for $\mathbf{L^1}$ can be deduced[20] for the three mononuclear species, the decomposition kinetics of which were monitored: $[CuH\mathbf{L^1}]^{3+}$, $[Cu\mathbf{L^1}]^{2+}$ and the one resulting from the rapid release of one Cu^{II} ion from the dinuclear complex. Although it is evident that a species such as $[CuH\mathbf{L^1}]^{3+}$ contains a protonated amine group that does not exist in $[Cu\mathbf{L^1}]^{2+}$, if the cyclophane is coordinated to the metal ion through the same donor groups in both complexes, the addition of the excess acid to a solution of $[Cu\mathbf{L^1}]^{2+}$ would lead to the formation of $[CuH\mathbf{L^1}]^{3+}$ within the mixing time of the stopped-flow instrument and the same kinetics of decomposition should be observed. This reasoning leads to the conclusion that $\mathbf{L^1}$ coordinates to the metal ion through the same number of donor atoms in both species (four according to the spectra and the equilibrium data) but the actual donor groups differ from one complex to the other. As protonation of the uncoordinated amine groups is faster than the breaking of Cu–N bonds, a species of composition $[CuH\mathbf{L^1}]^{3+}$ is rapidly formed when an excess of acid is added to a solution of $[Cu\mathbf{L^1}]^{2+}$ but this $[CuH\mathbf{L^1}]^{3+}$ species is an isomer of the most thermodynamically stable species with the same composition and so its kinetics of decomposition will be different. A similar reasoning can be applied to the mononuclear species formed as an intermediate during the decomposition of the dinuclear $[Cu_2\mathbf{L^1}(OH)_2]^{2+}$ complex. It appears unlikely that $\mathbf{L^1}$ coordinates to one of the metal centres in the dinuclear species through more than three amine groups but the lability of the Cu^{II} ion again makes possible the formation of a $[CuH\mathbf{L^1}]^{3+}$ species following the dissociation of the first metal ion. As this species decomposes with kinetics different from those observed in the study of the mononuclear species, it must be concluded that it is actually a different isomer. Thus, the different values of the *a* and *b* kinetics parameters obtained for solutions containing the $[CuH\mathbf{L^1}]^{3+}$, $[Cu\mathbf{L^1}]^{2+}$ and $[Cu_2\mathbf{L^1}(OH)_2]^{2+}$ complexes would actually correspond to the decomposition of three isomeric forms of the $[CuH\mathbf{L^1}]^{3+}$ species.

An attractive hypothesis is that the three species show the coordination environment depicted schematically in Figure 8. Independent of their precise structures, it can be anticipated that these isomers would have Cu–N bonds with different steric constrains that would lead to different kinetics of decomposition.[23,30–34] We have observed recently[7] these kinds of differences in the kinetics of decomposition for the mononuclear Cu^{II} complexes of cyclophanes with larger polyamine chains containing an additional amine group and suggested that these kinetic measurements are a useful test to detect changes in the actual coordination mode of the ligand. However, extensive DFT calculations indicated that the only way of getting a tetradentate coordination for $\mathbf{L^1}$ in mononuclear Cu^{II} complexes is by keeping one of the benzylic nitrogen atoms uncoordinated, i.e. as

shown in the structure at the right hand side of Figure 8. Thus, the experimental observation of different kinetics of decomposition for three species with the same set of donor atoms would reveal that the complex does not reorganise rapidly to the most stable conformation of $[CuH\mathbf{L^1}]^{3+}$ upon protonation of $[Cu\mathbf{L^1}]^{2+}$ or Cu^{II} dissociation from $[Cu_2\mathbf{L^1}(OH)_2]^{2+}$. In the latter cases, the rapid processes occurring within the mixing time of the stopped-flow instrument appear to lead to different conformations of the $[CuH\mathbf{L^1}]^{3+}$ species. If decomposition is faster than reorganisation to the most stable conformation, these transient species will decompose with different kinetics because of the different steric constraints of the Cu–N bonds in their coordination environments.

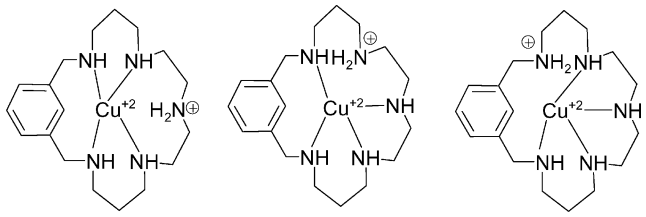

Figure 8. Schematic drawings showing three hypothetical isomeric forms of the $[CuH\mathbf{L^1}]^{3+}$ species with the $\mathbf{L^1}$ cyclophane acting as a tetradentate ligand. The actual coordination spheres can be more complex because of the presence of additional water ligands.

The comparison of the actual values of the kinetic parameters obtained in the present work with those previously reported for related complexes requires a previous consideration of the intimate mechanism of decomposition. The mechanism widely accepted in the literature[30–32] for the decomposition of polyamine complexes of Cu^{II} assumes that the acid attack on the Cu–N bond that is broken in the rate-determining step does not occur directly because it requires the previous formation of an activated intermediate "Cu–N" with partial breaking of the Cu–N bond [Equation (3)]. The complete dissociation of the metal–ligand bond can be achieved through two parallel pathways that involve solvent or acid attacks on this intermediate [Equations (4) and (5)]. If the activated intermediate is assumed to be formed under steady-state conditions the rate law for this mechanism is given by Equation (6) which can be simplified to the form of Equation (2) with the equivalences $a = k_1k_{H_2O}/(k_{-1} + k_{H_2O})$ and $b = k_1k_H/(k_{-1} + k_{H_2O})$, assuming that $k_H[H^+] << (k_{-1} + k_{H_2O})$. Thus, the b/a quotient is equivalent to k_H/k_{H_2O} and indicates the relative rates of attack by H^+ and H_2O on the activated intermediate.

$$Cu\text{–}N \leftrightarrows \text{“Cu–N”};\ k_1,\ k_{-1} \tag{3}$$

$$\text{“Cu–N”} + H_2O \rightarrow Cu^{2+} + HN^+;\ k_{H_2O} \tag{4}$$

$$\text{“Cu–N”} + H^+ \rightarrow Cu^{2+} + HN^+;\ k_H \tag{5}$$

$$k_{obs} = \frac{k_1k_{H_2O} + k_1k_H[H^+]}{k_{-1} + k_{H_2O} + k_H[H^+]} \tag{6}$$

For the decomposition of the Cu^{II} complexes with the open-chain polyamine $\mathbf{L^4}$,[19] the value of a is negligible and $b = 217\ M^{-1}s^{-1}$. Thus, although the macrocyclic nature of the $\mathbf{L^1}$ and $\mathbf{L^2}$ ligands only causes small changes in the values of b, the appearance of a significant a term indicates that the contribution of the solvent-attack pathway becomes more important for the complexes with both cyclophanes. However, for the Cu^{II} complexes with the pyridinophane $\mathbf{L^3}$,[19] a becomes negligible again, b is somewhat larger (520–700 $M^{-1}s^{-1}$) and the approximation $k_H[H^+] << (k_{-1} + k_{H_2O})$ is not valid, the plots of k_{obs} vs. $[H^+]$ showing a clear curvature that allows the calculation of a new parameter $c = k_H/(k_{-1} + k_{H_2O}) = 27\ M^{-1}$. Thus, the cyclic nature of the polyamine is not enough to cause the appearance of a significant a term in the kinetics of decomposition of the Cu^{II} complexes. The relative importance of both parallel attacks must then be better related to differences in the nature of the activated intermediate "Cu–N" which facilitates or hinders attacks by solvent and H^+, depending of the degree of bond dissociation. Solvent attack will be facilitated when the Cu–N bond becomes more elongated in the intermediate, whereas the assistance of H^+ is necessary when there is a small degree of bond dissociation. The extent to which the Cu–N bond is elongated in the intermediate appears to be determined by subtle changes in the steric constraints imposed by the ligand in the different species more than by the cyclic/acyclic nature of the polyamine. Thus, for the phenanthroline analogue of $\mathbf{L^1}$ and $\mathbf{L^2}$, the $[CuHL]^{3+}$ species decomposes mainly through the solvent-dependent pathway ($a = 18\ s^{-1}$, $b = 1.34\ M^{-1}s^{-1}$), whereas $[CuL]^{2+}$ decomposes exclusively through the H^+-pathway ($a = 0$, $b = 4264\ M^{-1}s^{-1}$, $c = 52\ M^{-1}$).[35]

Interaction with AMP and Formation of Ternary Cu^{II}–AMP-Cyclophane Complexes

To further explore the coordination properties of these new cyclophanes, additional studies were carried out on AMP recognition. The formation of mixed $[Cu_pH_rL(AMP)]^{(2p+r-2)+}$ complexes and especially their stability is of relevance in oligonucleotide binding,[12,36–38] and the present Cu–**L** systems (**L** = $\mathbf{L^1}$, $\mathbf{L^2}$, $\mathbf{L^3}$) offer an excellent opportunity for exploring the recognition capability in closely related mono- and dinuclear species.

A prerequisite for the determination of the constants of the mixed AMP–Cu^{II} complexes with $\mathbf{L^1}$, $\mathbf{L^2}$ and $\mathbf{L^3}$ is the knowledge of the stability constants of all the binary systems implicated. As polyammonium receptors can interact by themselves with nucleotide species, the equilibrium constants for the systems AMP–$\mathbf{L^1}$, AMP–$\mathbf{L^2}$ and AMP–$\mathbf{L^3}$ were determined potentiometrically and the values obtained for the global stability constants are included in Table 4. However, as both AMP and the **L** receptors participate in overlapping protonation processes, translating those cumulative constants into representative stepwise constants requires consideration of the basicity of AMP[39] and the different cyclophanes. If it is assumed that the interaction be-

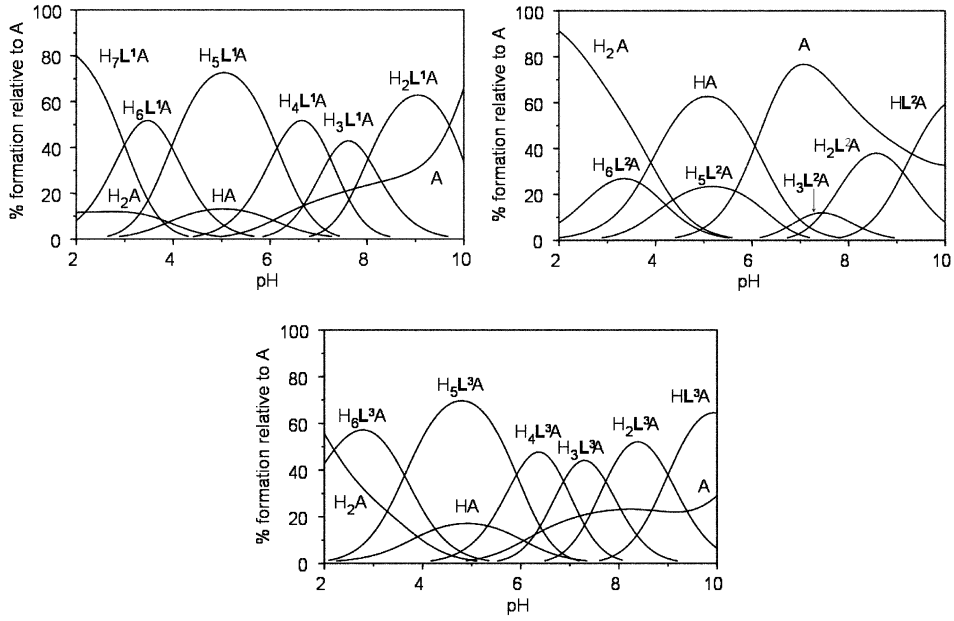

Figure 9. Species distribution curves for the **L**-A-H systems (**L** = **L^1**, **L^2**, **L^3**; A = AMP^{-2}; $[L]_0 = [A]_0 = 1 \times 10^{-3}$ M).

tween both species does not alter very much in the pH range in which the different protonated forms of AMP and **L** exist, the stepwise constants shown in the last part of Table 4 can be considered representative of the equilibria occurring in solution. Species distribution curves calculated from the equilibrium data in Table 4 are shown in Figure 9 which reveals that H_xL^{x+}-AMP species dominate at most pH values for the case of the **L^1** and **L^3** ligands, the interaction of the *para* **L^2** ligand being significantly lower. This is clearly reflected in a plot of the amount of complexed AMP (A) by the different receptors (A/L, 1:1 mole ratio) shown in Figure 10.

Table 4. Logarithms of the stability constants for the **L^1**–AMP, **L^2**–AMP and **L^3**–AMP species (A = AMP^{-2}) determined at 298.1 ± 0.1 K in 0.15 mol dm^{-3} $NaClO_4$.

Reaction[a]	**L^1**	**L^2**	**L^3**
A + L+ H = HLA	–	14.65(4)[b]	14.07(5)
A + L+ 2 H = H_2LA	22.37(1)	23.78(4)	23.07(5)
A + L+ 3 H = H_3LA	30.89(1)	31.24(9)	30.80(4)
A + L+ 4 H = H_4LA	38.47(1)	–	37.67(4)
A + L+ 5 H = H_5LA	44.84(1)	44.65(6)	43.59(4)
A + L+ 6 H = H_6LA	48.89(1)	48.87(6)	47.22(5)
A + L+ 7 H = H_7LA	51.46(2)	–	–
A + LH = HLA	–	3.96	4.42
A + LH_2 = H_2LA	3.30	3.43	4.10
A + LH_3 = H_3LA	4.01	2.57	4.21
A + LH_4 = H_4LA	4.59	–	4.46
AH + LH_4 = H_5LA	4.90	2.71	4.32
AH + LH_5 = H_6LA	6.16	3.90	5.09
AH_2 + LH_4 = H_6LA	5.05	3.03	4.05
AH_2 + LH_5 = H_7LA	4.83	–	–

[a] Charges omitted for clarity. [b] Values in parentheses are standard deviations in the last significant Figure.

In general, the values of the constants in Table 4 are of the same order as those found for the interaction of AMP with the protonated forms of some other polyaza macrocycles[36,38] and significantly higher than those found for smaller amines and for biogenic amines such as spermidine or putrescine.[8,40] It is also interesting to note that the stability of the AMP–H_xL species is also lower with polyaza macrocycles that are larger than the present cyclophanes.[41] This appears to show that the interaction is optimised for macrocycles of intermediate size in which the phosphate group better matches the positive charges of the macrocyclic cavity. In addition, the interaction probably becomes stronger for the case of cyclophanes because of additional π stacking interactions and actually, the stability constants found in this work are larger than those found for macrocycles of a similar size but lacking aromatic spacers.[8,36–40] Another interesting conclusion from the data in Table 4 is that the strength of the interaction between AMP^{2-} and the different H_xL^{x+} forms does not appear to be affected significantly when the positive charge on the cyclophane is in-

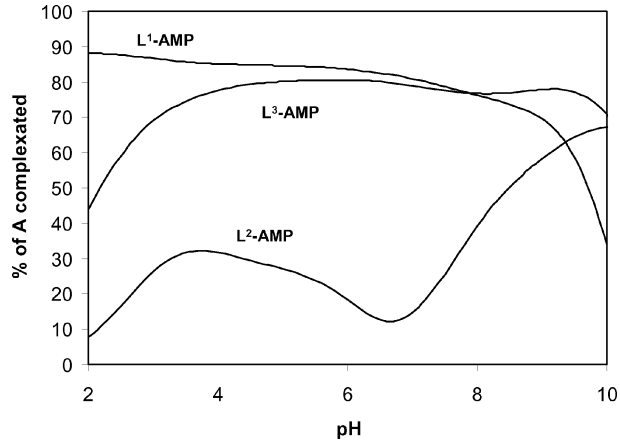

Figure 10. Plot of the percentage of complexed AMP for the three systems ([AMP] = 10^{-3} M).

creased which strongly suggests that the strength of the interaction is not dominated only by charge-charge electrostatic factors. Other factors like hydrogen bonding should also significantly affect the interaction. In this sense, it must be pointed out that although the stability of H_xL^{x+}-AMP adducts usually tends to increase with the protonation state of **L** because of the increased coulombic attractions and the larger number of possible hydrogen bonds between the host and the guest,[38,40,41] there are also literature reports showing similar stability constants for the interaction of AMP with the different protonated forms of some tripodal polyamines.[42]

The determination of the stability constants for the Cu–**L**-AMP systems (**L** = **L**^{1}, **L**^{2} and **L**^{3}) through the analysis of the titration curves is much more complex because of the large number of species present in solution. The analysis was carried out by fixing the values of the protonation constants of AMP,[39] the formation constants of the Cu^{2+}–AMP complexes[43] and the previously discussed protonation constants of the different **L** cyclophanes (Table 1), the equilibrium constants for the AMP–**L** system (Table 4) and those for the Cu–**L** complexes (Table 2). The results so obtained are included in Table 5 and representative species distribution curves are shown in Figure 10. Because of the complex nature of the equilibrium mixtures, the quality of these results was then checked by fitting together the data corresponding to titrations of binary Cu–**L** and ternary Cu–**L**-AMP systems including, as parameters to be refined, all the constants for the formation of Cu–**L** and Cu–**L**-AMP complexes. This analysis leads to results similar to those previously described, the differences being in all cases within the limits of the estimated errors.

Comparison of the data in Tables 4 and 5 indicates that the Cu^{II} complexes of the **L** cyclophanes show stability constants for the interaction with AMP quite similar to those observed for the protonated forms of the ligand, except for the case of the mononuclear complexes of **L**^{3}, the stability constants of which for the interaction with AMP are up to 4 log units higher than those found for the protonated ligand. However, it must be pointed out that the nature of the interaction between AMP and the receptor is presumably different in both cases because Cu–L complexes are coordinatively unsaturated and so they are susceptible to AMP coordination. At this point, it is interesting to note that all the log *K* values in Table 5 indicate that all the Cu–L complexes interact with AMP more strongly than Cu^{2+} (log $K_{Cu–AMP}$ = 3.0–3.2)[40,43–45] although the values can be considered to

Table 5. Logarithms of the stability constants for the formation of mixed Cu–**L**-AMP complexes (AMP^{-2} = A) determined at 298.1 ± 0.1 K in 0.15 mol dm^{-3} $NaClO_4$.

Reaction[a]	**L**^{1}	**L**^{2}	**L**^{3}
Cu + L + A = CuLA	23.5(1)[b]	–	–
Cu + H + L + A = CuHLA	31.2(1)[b]	–	34.08(6)
Cu + 2 H + L + A = CuH_2LA	37.89(1)	36.00 (3)	40.55(6)
Cu + 3 H + L + A = CuH_3LA	41.56(2)	40.41(10)	44.53(7)
Cu + 4 H + L + A = CuH_4LA	–	45.18 (4)	47.88(7)
2 Cu + L + A = Cu_2LA	–	27.78 (4)	33.73(7)
2 Cu + H + L + A = Cu_2HLA	–	–	38.80(1)
2 Cu + 2 H + L + A = Cu_2H_2LA	–	39.93(4)	–
2 Cu + L + A = Cu_2LA	29.09(2)	–	–
2 Cu + H_2O + L + A = $Cu_2LA(OH)$ + H	22.00(2)	20.61(5)	24.80(1)
CuH_3L + AH = CuH_4LA	–	3.98	–
CuH_2L + AH_2 = CuH_4LA	–	4.07	7.77
CuH_2L + AH = CuH_3LA	5.87	3.53	8.32
CuHL + AH_2 = CuH_3LA	5.30	4.75	7.17
CuHL + AH = CuH_2LA	5.53	4.24	7.09
CuHL + A = CuHLA	4.90	–	6.68
$Cu_2L(OH)$ + A = $Cu_2LA(OH)$	–	5.42	4.10

[a] Charges omitted for clarity. [b] Values in parentheses are standard deviations in the last significant Figure.

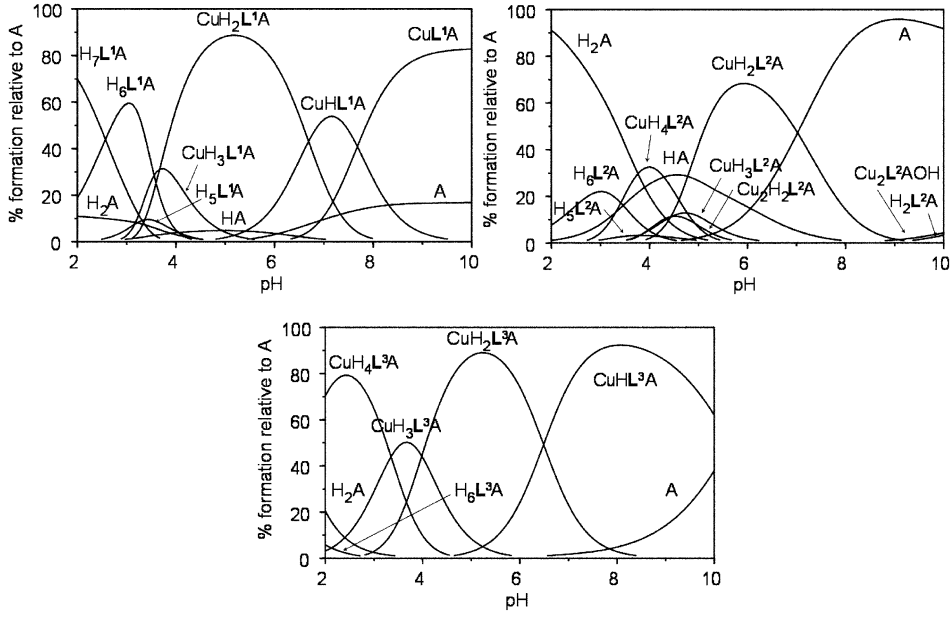

Figure 11. Species distribution diagrams for the mixed Cu–**L**-A-H systems (**L** = **L**^{1}, **L**^{2}, **L**^{3}; A = AMP^{-2}; $[Cu^{+2}] = [L]_0 = [A]_0 = 1 \times 10^{-3}$ M).

be similar to those found for other Cu–polyamine complexes.[40,41,46] The stability of the interactions with mononuclear Cu–**L³** complexes are among the most stable. These results, and especially the large stabilisation observed for the **L³** complexes, strongly suggest that selectivity in recognition is probably determined more by other interactions (hydrogen bonding, π stacking) than by direct coordination to the metal centre.

However, because of the existence of multiple competitive equilibria, we have plotted the percentages of complexed AMP as a function of pH for both systems in order to better compare the affinity for AMP of the free ligands and their protonated complexes with that that displayed by the Cu^{II}–L complexes (see Figure 11 and Supporting Information). While for the systems AMP–**L¹** and AMP–**L³** Cu^{II} addition does not yield large increases in the amount of complexed AMP, in the case of the *para* derivative **L²** the amount of complexed AMP in the presence of Cu^{II} is clearly augmented over a broad pH range (Figure 12).

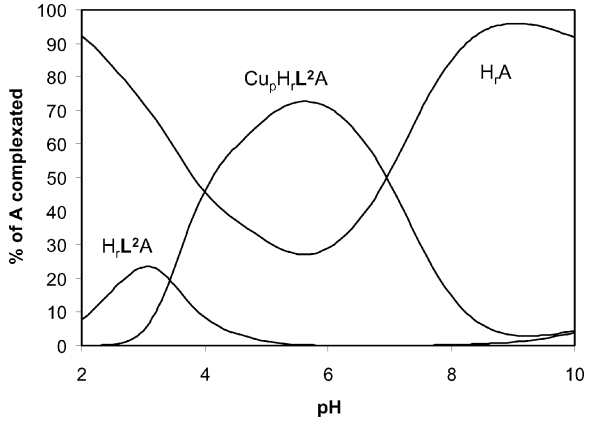

Figure 12. Percentages of complexed AMP for the system Cu^{II}–AMP-L calculated for 1:1:1 molar ratio ([AMP] = 1×10^{-3} M).

Experimental Section

Syntheses

2,6,9,12,16-Pentakis(*p*-tolylsulfonyl)-2,6,9,12,16-pentaza[17]metacyclophane (L1·5Ts): A solution of α,α′-dibromo-*m*-xylene (2.03 g, 7.67 mmol) in a dry CH_3CN/CH_2Cl_2 (1:1 v/v, 150 mL) mixture was added dropwise to a suspension of 1,5,8,11,15-pentakis(*p*-tolylsulfonyl)-1,5,8,11,15-pentazapentadecane (7.60 g, 7.67 mmol) and K_2CO_3 (10.55 g, 76.3 mmol) in dry CH_3CN (250 mL). The suspension was heated to reflux for a further 24 h and then filtered. The resultant solution was vacuum-evaporated to dryness and the residue suspended in ethanol at reflux to give **L1·5Ts** as a white solid (2.79 g, yield 37%); m.p. 108–110 °C. $C_{53}H_{63}N_5O_{10}S_5$ (1090.41): calcd. C 58.38, H 5.82, N 6.42; found C 58.1, H 5.9, N 6.1. ^{1}H NMR ($CDCl_3$): δ = 1.74–1.76 (m, 4 H), 2.42 (s, 6 H), 2.44 (s, 6 H), 2.46 (s, 3 H), 3.03–3.09 (m, 8 H), 3.15–3.20 (t, J = 8 Hz, 4 H), 3.26–3.29 (t, J = 8 Hz, 4 H), 4.25 (s, 4 H), 7.25–7.28 (d, J = 8 Hz, 4 H), 7.28–7.31 (d, J = 8 Hz, 4 H), 7.32–7.35 (d, J = 8 Hz, 2 H), 7.37 (s, 3 H), 7.48 (s, 1 H), 7.61–7.63 (d, J = 8 Hz, 4 H), 7.68–7.71 (d, J = 8 Hz, 4 H), 7.73–7.76 (d, J = 8 Hz, 2 H) ppm. ^{13}C NMR ($CDCl_3$): δ = 19.1, 26.9, 45.8, 46.2, 46.4, 47.2, 51.5, 124.8, 125.1, 127.5, 127.6, 135.7, 141.2 ppm. MS (FAB): m/z = 1090 [M^+].

2,6,9,12,16-Pentakis(*p*-tolylsulfonyl)-2,6,9,12,16-pentaza[17]paracyclophane (L²·5Ts): This compound was obtained using the procedure described for **L¹·5Ts** except that α,α′-dibromo-*p*-xylene was used instead of α,α′-dibromo-*m*-xylene. The product was also isolated as a white solid (5.53 g, yield 67%); m.p. 187–189 °C. $C_{53}H_{63}N_5O_{10}S_5$ (1090.41): calcd. C 58.38, H 5.82, N 6.42; found C 58.3, H 5.9, N 6.5. ^{1}H NMR ($CDCl_3$): δ = 1.57–1.63 (m, 4 H), 2.42 (s, 12 H), 2.46 (s, 3 H), 2.91–3.11 (m, 16 H), 4.19 (s, 4 H), 7.17 (s, 4 H), 7.29 (d, J = 8 Hz, 8 H), 7.33 (d, J = 8 Hz, 4 H), 7.63 (d, J = 8 Hz, 8 H), 7.72 (d, J = 8 Hz, 4 H) ppm. ^{13}C NMR ($CDCl_3$): δ = 19.2, 26.8, 45.4, 46.2, 46.6, 48.0, 51.2, 124.9, 125.0, 125.8, 127.5, 127.6, 132.8, 133.6, 134.1, 138.6, 141.2, 141.7 ppm. MS (FAB): m/z = 1089 [M – H]$^+$.

2,6,9,12,16-Pentaza[17]metacyclophane Pentahydrochloride (L¹·5HCl): The tosyl groups of **L¹·5Ts** (2.79 g, 2.56 mmol) were removed by reductive cleavage with a mixture of HBr/HAc (150 mL) and PhOH (15.20 g, 16.0 mmol) by heating at 90 °C for 24 h. The solid obtained was then filtered and washed with a mixture of EtOH/CH_2Cl_2 (1:1 v/v). The macrocycle was obtained as its hydrobromide salt and was then converted into the free amine by using an ionic exchange resin (Amberlite IRA 402). The free amine was purified by chromatography on neutral alumina using methanol as the eluent. The resultant oil was dissolved in ethanol and treated with 37% HCl until complete precipitation of a white solid which was filtered to give **L¹** as its pentahydrochloride salt (0.45 g, yield 35%); m.p. 185–187 °C. $C_{18}H_{33}N_5 \cdot 5HCl \cdot 3H_2O$ (555.84): calcd. C 38.90, H 7.98, N 12.60; found C 39.0, H 8.0, N 12.6. ^{1}H NMR (D_2O): δ = 1.85–1.95 (m, 4 H), 2.95–2.98 (m, 8 H), 3.22 (s, 8 H), 4.04 (s, 4 H), 7.28 (s, 3 H), 7.37 (s, 1 H) ppm. ^{13}C NMR (D_2O): δ = 23.2, 43.9, 44.1, 44.4, 44.9, 51.1, 130.5, 131.3, 131.6, 132.8 ppm.

2,6,9,12,16-Pentaza[17]paracyclophane Pentahydrochloride (L²·5HCl): This compound was obtained from **L²·5Ts** using the same procedure described above for the analogous metacyclophane (0.68 g, yield 33%); m.p. 248–250 °C. $C_{18}H_{33}N_5 \cdot 5HCl \cdot 3H_2O$ (555.84): calcd. C 38.90, H 7.98, N 12.60; found C 39.3, H 8.0, N 12.6. ^{1}H NMR (D_2O): δ = 1.66–1.75 (m, 4 H), 2.68–2.70 (m, 4 H), 2.75–2.85 (m, 12 H), 4.04 (s, 4 H), 7.41 (s, 4 H) ppm. ^{13}C NMR (D_2O): δ = 23.2, 43.1, 44.6, 45.2, 50.6, 131.4, 131.6 ppm.

EMF Measurements: The potentiometric titrations were carried out at 298.1 ± 0.1 K using 0.15 M $NaClO_4$ as the supporting electrolyte. The experimental procedure (burette, potentiometer, cell, stirrer, microcomputer, etc.) has been fully described elsewhere.[47] The acquisition of the emf data was carried out with the computer program PASAT.[48] The reference electrode was an Ag/AgCl electrode in saturated KCl solution. The glass electrode was calibrated as a hydrogen-ion concentration probe by titration of previously standardised amounts of HCl with CO_2-free NaOH solutions and determination of the equivalent point by the Gran's method[49] which gives the standard potential E^0 and the ionic product of water [pK_w = 13.73(1)].

The computer program HYPERQUAD was used to calculate the protonation and stability constants from the titration curves.[50] The protonation constants for AMP were taken from ref.[12]. The pH range investigated was 2.5–10.5 and the concentration of Cu^{II}, AMP and ligands ranged from 3×10^{-4} to a maximum value of 1.5×10^{-3} mol dm^{-3}. The different titration curves for each system (at least two) were treated either as a single set or as separated curves without significant variations in the values of the stability constants. The sets of data were merged together and treated simultaneously to give the final stability constants. Moreover, in the case of the AMP–L systems several measurements were made both in

formation and in dissociation (from acid to alkaline pH and vice versa) to check the reversibility of the reactions.

DFT Calculations: All DFT calculations were performed using the Gaussian03 package[51] and the unrestricted Becke three-parameter hybrid functional combined with the Lee–Yang–Parr correlation functional (UB3LYP).[52,53] The Pople style 6-31G(d,p) basis set was used on the C, H, O and N atoms, and the SDD basis set[54] and effective core potential (ECP) on Cu (as implemented in Gaussian03, SDD is D95V up to Ar and Stuttgart/Dresden ECPs for the remaining elements of the periodic Table). All geometry optimisations were performed without any symmetry constrains and efforts were made to find the lowest energy conformation by comparing the structures optimised from different starting geometries. Harmonic frequency calculations were performed to confirm that the calculated structures were minima. Aqueous solution energies were calculated using the CPCM formalism[55,56] (water solvent, $\varepsilon = 78.39$ as implemented in Gaussian03). The gas phase geometry was used for all of these calculations because it has been demonstrated in many previous studies that the change of geometry due to solvation effects is usually insignificant.[57,58]

Kinetic Experiments: The kinetics of decomposition of the Cu^{II} complexes with the ligands $\mathbf{L^1}$ and $\mathbf{L^2}$ were studied at 298.1 ± 0.1 °C using an Applied Photophysics SX17MV stopped-flow spectrophotometer. The Cu/L ligand ratio and the pH of the starting solutions of the metal complexes were selected from the species distribution curves in order to achieve the maximum concentration for one of the complex species while maintaining a very low concentration of the others. For this reason, only those species which represent at least 80% of the total ligand under some conditions were studied. These solutions were mixed in the stopped-flow instrument with solutions containing $HClO_4$ at the desired concentration. The ionic strength of both solutions was adjusted to 0.15 M with $NaClO_4$. The decomposition of the $\mathbf{L^1}$ and $\mathbf{L^2}$ complexes was monitored at 575 nm and 610 nm, respectively, because the absorbance changes observed in preliminary experiments using a diode-array detector were at a maximum at these wavelengths. In all cases, the data for the acid-promoted decomposition of the complexes could be satisfactorily fitted by a single exponential using the software of the stopped-flow instrument. The data from the preliminary diode-array experiments were analysed with the GLINT program[59] and yielded rate constants similar to those derived from the single-wavelength experiments in addition to the spectra of the reaction mixture immediately after mixing and at the end of the decomposition process.

Supporting Information (see footnote on the first page of this article): Additional species distribution curves, EPR spectra, Cartesian coordinates, geometries and energies of all the species optimized by DFT procedures.

Acknowledgments

We would like to acknowledge Ministerio de Ciencia y Tecnología (MCYT) and the Federación Española de Enfermedades Raras (FEDER) (Grants CTQ2006-14909-C02-01 and CTQ2006-15672-CO5-01) as well as the Junta de Andalucía (FQM-137) for financial support. Computer facilities by the Centro de Supercomputación de la Universidad de Cádiz are also acknowledged. Predoctoral grants are also acknowledged to Ayuntamiento de Valencia (to B. V.), Universidad de Cádiz (to C. E. C.), and MCYT (to S. B. and A. G. A.).

[1] a) A. Bencini, M. I. Burguete, E. García-España, S. V. Luis, J. F. Miravet, C. Soriano, *J. Org. Chem.* **1993**, *58*, 4749–4753; b) M. I. Burguete, B. Escuder, E. García-España, S. V. Luis, J. F. Miravet, *J. Org. Chem.* **1994**, *59*, 1067–1071; c) B. Altava, M. I. Burguete, B. Escuder, E. García-España, M. C. Muñoz, *Tetrahedron* **1997**, *53*, 2629–2640.

[2] a) A. Andrés, M. I. Burguete, E. García-España, S. V. Luis, J. F. Miravet, C. Soriano, *J. Chem. Soc. Perkin Trans. 2* **1993**, 749–755; b) E. García-España, J. Latorre, S. V. Luis, J. F. Miravet, P. Pozuelo, J. A. Ramírez, C. Soriano, *Inorg. Chem.* **1996**, *35*, 4591–4596; c) B. Altava, A. Bianchi, C. Bazzicalupi, M. I. Burguete, E. García-España, S. V. Luis, J. F. Miravet, *Supramol. Chem.* **1997**, *8*, 287–299; d) J. A. Aguilar, P. Díaz, A. Doménech, E. García-España, J. M. Llinares, S. V. Luis, J. A. Ramírez, C. Soriano, *J. Chem. Soc. Perkin Trans. 2* **1999**, 1159–1168; e) M. I. Burguete, P. Díaz, E. García-España, S. V. Luis, J. F. Miravet, M. Querol, J. A. Ramírez, *Chem. Commun.* **1999**, 649–650.

[3] A. Andrés, C. Bazzicalupi, A. Bianchi, E. García-España, S. V. Luis, J. F. Miravet, J. A. Ramírez, *J. Chem. Soc., Dalton Trans.* **1994**, 2995–3004.

[4] M. I. Burguete, B. Escuder, E. García-España, J. Latorre, S. V. Luis, J. A. Ramírez, *Inorg. Chim. Acta* **2000**, *300*, 970–977.

[5] B. Altava, M. I. Burguete, S. V. Luis, J. F. Miravet, E. García-España, V. Marcelino, C. Soriano, *Tetrahedron* **1997**, *53*, 4751–4762.

[6] M. I. Burguete, E. García-España, S. V. Luis, J. F. Miravet, C. Soriano, *An. Quím.* **1993**, *89*, 99–100.

[7] J. Aguilar, M. G. Basallote, L. Gil, J. C. Hernández, M. A. Máñez, E. García-España, C. Soriano, B. Verdejo, *Dalton Trans.* **2004**, 94–103.

[8] E. Kimura, M. Kodama, T. Yatsunami, *J. Am. Chem. Soc.* **1982**, *104*, 3182–3187.

[9] M. W. Hosseini, J. M. Lehn, M. P. Mertes, *Helv. Chim. Acta* **1983**, *66*, 2454–2466.

[10] B. Dietrich, M. W. Hosseini, J. M. Lehn, R. B. Sessions, *J. Am. Chem. Soc.* **1981**, *103*, 1282–1283.

[11] M. W. Hosseini, J. M. Lehn, *Helv. Chim. Acta* **1987**, *70*, 1312–1319.

[12] A. Bencini, A. Bianchi, E. García-España, E. C. Scott, L. Morales, B. Wang, T. Deffo, F. Takusagawa, M. P. Mertes, K. B. Mertes, P. Paoletti, *Bioorg. Chem.* **1992**, *20*, 8–29.

[13] For a recent review on ATP coordination by polyazamacrocycles see for instance: E. García-España, P. Díaz, J. M. Llinares, A. Bianchi, *Coord. Chem. Rev.* **2006**, *250*, 2952–2987.

[14] E. Martell, R. J. Motekaitis, Q. Lu, D. A. Nation, *Polyhedron* **1999**, *18*, 3203–3218.

[15] Szymanska, H. Radecka, J. Radecki, M. Pietraszkiewicz, O. Pietraszkiewicz, *Comb. Chem. High Throughput Screening* **2000**, *3*, 509–517.

[16] S. Y. Lin, W. H. Chen, C. Y. Liu, *Electrophoresis* **2002**, *23*, 3550–3557.

[17] M. T. Albelda, J. Aguilar, S. Alves, R. Aucejo, P. Díaz, C. Lodeiro, J. C. Lima, E. García-España, F. Pina, C. Soriano, *Helv. Chim. Acta* **2003**, *86*, 3118–3135.

[18] J. A. Aguilar, P. Díaz, F. Escartí, E. García-España, L. Gil, C. Soriano, B. Verdejo, *Inorg. Chim. Acta* **2002**, *339*, 307–316.

[19] P. Díaz, M. G. Basallote, M. A. Máñez, E. García-España, L. Gil, J. Latorre, C. Soriano, B. Verdejo, S. V. Luis, *Dalton Trans.* **2003**, 1186–1193.

[20] H. Gampp, D. Haspra, M. Maeder, A. D. Zuberbuehller, *Inorg. Chem.* **1984**, *23*, 3724–3730.

[21] S. Siddiqui, R. E. Shepherd, *Inorg. Chem.* **1986**, *25*, 3869–3876.

[22] See for instance: a) E. Kimura, I. Nakamura, T. Koike, M. Shionoya, Y. Kodama, T. Ikeda, M. Shiro, *J. Am. Chem. Soc.* **1994**, *116*, 4764–4771; b) T. Koike, S. Kajitani, I. Nakamura, E. Kimura, M. Shiro, *J. Am. Chem. Soc.* **1995**, *117*, 1210–1219; c) C. Bazzigalupi, A. Bencini, E. Berni, S. Ciattini, A. Bianchi,

C. Giorgi, P. Paoletti, B. Valtancoli, *Inorg. Chim. Acta* **2001**, *317*, 259–267.
[23] L. H. Chen, C. S. Chung, *Inorg. Chem.* **1989**, *28*, 1402–1405.
[24] See for example: a) T. G. Fawcett, S. M. Rudich, B. H. Toby, R. A. Lalancette, J. A. Potenza, H. J. Schugar, *Inorg. Chem.* **1980**, *19*, 940–945; b) Z. D. Georgousis, P. C. Christidis, D. Hadjipavlou-Litina, C. A. Bolos, *J. Mol. Struct.* **2007**, *837*, 30–37; c) M. Chadim, P. Díaz, E. García-España, J. Hodacova, P. C. Junk, J. Latorre, J. M. Llinares, C. Soriano, J. Zavada, *New J. Chem.* **2003**, *27*, 1132–1139; d) A. T. Chaviara, P. C. Christidis, A. Papageorgiou, E. Chrysogelou, D. J. Hadjipavlou-Litina, C. A. Bolos, *J. Inorg. Biochem.* **2005**, *99*, 2102–2109; e) P. Antunes, R. Delgado, M. G. B. Drew, V. Félix, H. Maecke, *Inorg. Chem.* **2007**, *46*, 3144–3153.
[25] R. J. Deeth, *J. Chem. Soc., Dalton Trans.* **2001**, 664–669.
[26] M. G. Basallote, J. Durán, M. J. Fernández-Trujillo, M. A. Máñez, *J. Chem. Soc., Dalton Trans.* **1999**, 3817–3823.
[27] M. G. Basallote, J. Durán, M. J. Fernández-Trujillo, M. A. Máñez, *Polyhedron* **2001**, *20*, 75–82.
[28] M. G. Basallote, J. Durán, M. J. Fernández-Trujillo, M. A. Máñez, M. Quirós, J. M. Salas, *Polyhedron* **2001**, *20*, 297–305.
[29] M. G. Basallote, J. Durán, M. J. Fernández-Trujillo, M. A. Máñez, *J. Chem. Soc., Dalton Trans.* **2002**, 2074–2079.
[30] R. A. Read, D. W. Margerum, *Inorg. Chem.* **1981**, *20*, 3143–3149.
[31] R. W. Hay, M. P. Pujari, R. Bembi, *Transition Met. Chem.* **1986**, *11*, 261–264.
[32] M. J. Fernández-Trujillo, B. Szpoganicz, M. A. Máñez, L. T. Kist, M. G. Basallote, *Polyhedron* **1996**, *15*, 3511–3517.
[33] S. Siddiqui, R. E. Shepherd, *Inorg. Chem.* **1983**, *22*, 3726–3733.
[34] L. H. Chen, C. S. Chung, *Inorg. Chem.* **1988**, *27*, 1880–1883.
[35] A. Mendoza, J. Aguilar, M. G. Basallote, L. Gil, J. C. Hernández, M. A. Máñez, E. García-España, L. Ruiz-Ramírez, C. Soriano, B. Verdejo, *Chem. Commun.* **2003**, 3032–3033.
[36] a) M. W. Hosseini, J.-M. Lehn, M. P. Mertes, *Helv. Chim. Acta* **1983**, *66*, 2454–2466; b) B. Dietrich, M. W. Hosseini, J.-M. Lehn, R. B. Sessions, *Helv. Chim. Acta* **1985**, *68*, 289–299; c) M. W. Hosseini, J.-M. Lehn, *J. Chem. Soc., Chem. Commun.* **1985**, 1155–1157; d) M. W. Hosseini, J.-M. Lehn, L. Maggiora, K. B. Mertes, M. P. Mertes, *J. Am. Chem. Soc.* **1987**, *109*, 537–544; e) P. G. Yohannes, K. E. Plute, M. P. Mertes, K. B. Mertes, *Inorg. Chem.* **1987**, *26*, 1751–1755; f) M. W. Hosseini, J.-M. Lehn, *J. Am. Chem. Soc.* **1987**, *109*, 7047–7058; g) H. Jahansouz, Z. Jiang, R. H. Himes, M. P. Mertes, K. B. Mertes, *J. Am. Chem. Soc.* **1985**, *107*, 8288–8289; h) R. C. Bethel, G. Lowe, M. W. Hosseini, J.-M. Lehn, *Bioorg. Chem.* **1988**, *16*, 418–428; i) G. M. Blackburn, G. R. J. Thatcher, M. W. Hosseini, J.-M. Lehn, *Tetrahedron Lett.* **1987**, *28*, 2779–2782; j) Z. Jiang, P. Chalabi, K. B. Mertes, H. Jahansouz, R. H. Himes, M. P. Mertes, *Bioorg. Chem.* **1989**, *17*, 313–329; k) M. W. Hosseini, A. J. Blacker, J.-M. Lehn, *J. Am. Chem. Soc.* **1990**, *112*, 3896–3904; l) A. V. Eliseev, H.-J. Schneider, *J. Am. Chem. Soc.* **1994**, *116*, 6081–6088.
[37] a) J. Aguilar, E. García-España, J. Guerrero, S. V. Luis, J. M. Llinares, J. F. Miravet, J. A. Ramírez, C. Soriano, *J. Chem. Soc., Chem. Commun.* **1995**, 2237–2239; b) J. Aguilar, E. García-España, J. A. Guerrero, S. V. Luis, J. M. Llinares, J. A. Ramírez, C. Soriano, *Inorg. Chim. Acta* **1996**, *246*, 287–294; c) J. Aguilar, B. Celda, V. Fusi, E. García-España, S. V. Luis, M. C. Martínez, J. A. Ramírez, C. Soriano, R. Tejero, *J. Chem. Soc. Perkin Trans. 2* **2000**, *7*, 1323–1328; d) J. Aguilar, A. B. Descalzo, P. Díaz, V. Fusi, E. García-España, S. V. Luis, M. Micheloni, J. A. Ramírez, P. Romani, C. Soriano, *J. Chem. Soc. Perkin Trans. 2* **2000**, *6*, 1187–1192.
[38] a) R. Hettich, H. J. Schneider, *J. Am. Chem. Soc.* **1997**, *119*, 5638–5647; b) S. Borah, M. S. Melvin, N. Lindquist, R. A. Manderville, *J. Am. Chem. Soc.* **1998**, *120*, 4557–4562.
[39] A. E.Martell, R. M. Smith, R. J. Motekaitis, *NIST Critically Selected Stability Constants of Metal Complexes Database*, NIST Standard Reference Database, version 4, (**1997**).
[40] a) A. Gasowska, L. Lomozik, R. Jastrzab, *J. Inorg. Biochem.* **2000**, *78*, 139–147; b) L. Lomozik, A. Gasowska, G. Krzysko, *J. Inorg. Biochem.* **2006**, *100*, 1781–1789.
[41] a) C. Anda, A. Llobet, V. Salvado, J. Reibenspies, R. J. Motekaitis, A. E. Martell, *Inorg. Chem.* **2000**, *39*, 2986–2999; b) C. Anda, A. Llobet, V. Salvado, A. E. Martell, R. J. Motekaitis, *Inorg. Chem.* **2000**, *39*, 3000–3008.
[42] M. T. Albelda, E. García-España, H. R. Jiménez, J. M. Llinares, C. Soriano, A. Sornosa-Ten, B. Verdejo, *Dalton Trans.* **2006**, 4474–4481.
[43] E. M. Bianchi, S. A. A. Sajadi, B. Song, H. Sigel, *Chem. Eur. J.* **2003**, *9*, 881–892.
[44] H. Sigel, S. S. Massoud, N. A. Corfú, *J. Am. Chem. Soc.* **1994**, *116*, 2958–2971.
[45] S. S. Massoud, R. Tribolet, H. Sigel, *Eur. J. Biochem.* **1990**, *187*, 387–393.
[46] A. E. Martell, R. J. Motekaitis, Q. Lu, D. A. Nation, *Polyhedron* **1999**, *18*, 3203–3218.
[47] E. García-España, M. J. Ballester, F. Lloret, J. M. Moratal, J. Faus, A. Bianchi, *J. Chem. Soc., Dalton Trans.* **1988**, 101–104.
[48] M. Fontanelli, M. Micheloni, *Proceedings of the I Spanish-Italian Congress on Thermodynamics of metal complexes*, Diputación de Castellón, Castellón, Spain, **1990**. Program for the automatic control of the microburette and the acquisition of the electromotive force readings.
[49] a) G. Gran, *Analyst (London)* **1952**, *77*, 661–671; b) F. I. Rossotti, H. Rossotti, *J. Chem. Educ.* **1965**, *42*, 375.
[50] P. Gans, A. Sabatini, A. Vacca, *Talanta* **1996**, *43*, 1739–1753.
[51] M. J. Frisch, G. W. Trucks, H. B. Schlegel, G. E. Scuseria, M. A. Robb, J. R. Cheeseman, J. A. Montgomery, T. Vreven, K. N. Kudin, J. C. Burant, J. M. Millam, S. S. Iyengar, J. Tomasi, V. Barone, B. Mennucci, M. Cossi, G. Scalmani, N. Rega, G. H. Petersson, H. Nakatsuji, M. Hada, M. Ehara, K. Toyota, R. Fukuda, J. Hasegawa, M. Ishida, T. Nakajima, Y. Honda, O. Kitao, H. Nakai, M. Klene, X. Li, J. E. Knox, H. P. Hratchian, J. B. Cross, C. Adamo, J. Jaramillo, R. Gomperts, R. E. Stratmann, O. Yazyev, A. J. Austin, R. Cammi, C. Pomelli, J. W. Ochterski, P. Y. Ayala, K. Morokuma, G. A. Voth, P. Salvador, J. J. Dannenberg, V. G. Zakrzewski, S. Dapprich, A. D. Daniels, M. C. Strain, O. Farkas, D. K. Malick, A. D. Rabuck, K. Raghavachari, J. B. Foresman, J. V. Ortiz, Q. Cui, A. G. Baboul, S. Clifford, J. Cioslowski, B. B. Stefanov, G. Liu, A. Liashenko, P.Piskorz, I. Komaromi, R. L. Martin, D. J. Fox, T. Keith, M. A. Al-Laham, C. Y. Peng,;A. Nanayakkara, M.Challacombe, P. M. W. Gill, B. Johnson, W. Chen, M. W.Wong, C. Gonzalez, J. A. Pople, *Gaussian 03, Revision E.01*, Gaussian, Inc., Pittsburgh PA, **2003**.
[52] A. D. Becke, *J. Chem. Phys.* **1993**, *98*, 5648–5652.
[53] C. T. Lee, W. T. Yang, R. G. Parr, *Phys. Rev. B* **1988**, *37*, 785–789.
[54] D. Andrae, U. Haussermann, M. Dolg, H. Stoll, H. Preuss, *Theor. Chim. Acta* **1990**, *77*, 123–141.
[55] V. Barone, M. Cossi, *J. Phys. Chem. A* **1998**, *102*, 1995–2001.
[56] M. Cossi, N. Rega, G. Scalmani, V. Barone, *J. Comput. Chem.* **2003**, *24*, 669–681.
[57] C. J. Cramer, D. G. Truhlar, *Chem. Rev.* **1999**, *99*, 2161–2200.
[58] J. Tomasi, B. Mennucci, R. Cammi, *Chem. Rev.* **2005**, *105*, 2999–3093.
[59] GLINT Software, *Applied Photophysics Ltd.*, Leatherhead, U. K., **1997**.

Received: June 8, 2008
Published Online: November 28, 2008

